

Synthesis and Structure of Bimetallic Nickel Molybdenum Phosphide Solid Solutions

Ding Ma,[†] Tiancun Xiao,[†] Songhai Xie,^{‡,§}
Wuzong Zhou,[‡] Sergio L. Gonzalez-Cortes,[†] and
Malcolm L. H. Green^{*,†,||}

*Inorganic Chemistry Laboratory, Oxford University,
South Parks Road, Oxford, OX1 3QR, United
Kingdom, School of Chemistry, University of St.
Andrews, St. Andrews, KY16 9ST, United Kingdom,
and Department of Chemistry, Fudan University,
Shanghai 200433, China*

Received November 27, 2003

Revised Manuscript Received May 28, 2004

Catalysts for the petroleum industry such as transition metal sulfides, carbides, and nitrides have been extensively studied since the 1970s and especially during the past decade.¹ They can be efficient catalysts for hydrotreating reactions, and for Fischer–Tropsch synthesis,² and may even be used as catalysts for the oxidation reforming of methane.³ The depletion of conventional oil resources has led to a focus on heavy crude oil as the primary source of hydrocarbon fuels. For this reason there is a growing need to develop a new generation of hydrotreating catalysts suitable for the processing of heavy crude oil.

Recently, considerable attention has been drawn to the discovery that transition metal phosphides can have high performance in a hydrodenitrogenation (HDN) reaction.^{4–7} Weber and co-workers have shown that the intrinsic HDN (propylaniline) activity of surface Mo atoms of MoP was 6 times higher than that of conventional supported MoS₂ catalyst.^{6a} Very recently, ternary phosphides NiMoP and CoMoP have been shown to have interesting catalytic properties.⁸ Meanwhile, nickel-based catalysts have long been known to act as active hydrogenation catalysts, especially when combined with other metals as promoters.⁹ Therefore, in light of the

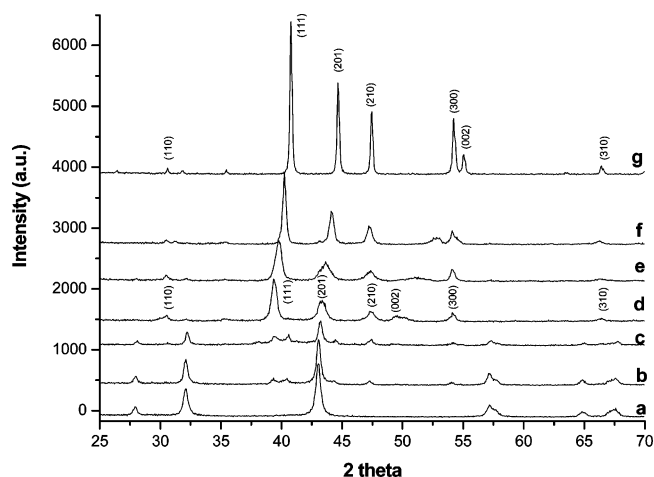


Figure 1. XRD patterns from (a) MoP, (b) Ni_{0.4}Mo_{1.6}P_{1.6} (nominal), (c) Ni_{0.66}Mo_{1.34}P_{1.34} (nominal), (d) NiMoP, (e) Ni_{1.34}Mo_{0.66}P, (f) Ni_{1.6}Mo_{0.4}P, and (g) Ni₂P. Both (d) and (g) are indexed onto the Fe₂P-type unit cells.

recently established activity of NiMo phosphides, we have set out to explore the possibility of the preparation of the unknown NiMo solid solutions with a variable Ni/Mo ratio. Since Ni₂P and NiMoP both have an Fe₂P type structure, a series of Ni_(2-x)Mo_xP ($x = 0–1$) solid solutions were anticipated and indeed have been prepared and characterized as described below.

The new materials were prepared using the following general procedure. A measured amount (chosen according to the stoichiometry of the aimed solids) of nickel nitrate Ni(NO₃)₂·6H₂O (BDH), ammonium heptamolybdate (AHM) (NH₄)₆Mo₇O₂₄·4H₂O (Riedel-de Haen), and diammonium hydrogen phosphate (NH₄)₂HPO₄ (Aldrich) were used as received. Each salt was dissolved separately in a small beaker with deionized water. Clear solutions were formed after continuous stirring. Afterward, the nickel nitrate solution or ammonium heptamolybdate solution (the former is for Ni₂P while the latter is for MoP, both of which are dissolved with deionized water) was added to the diammonium hydrogen phosphate solutions respectively under stirring. For the preparation of nominal compositions of NiMoP, Ni_(2-x)Mo_xP ($x = 0–1$), and Ni_xMo_(2-x)P_(2-x) ($x = 0–1$), a solution containing a mixture of AHM and diammonium hydrogen phosphate was first prepared and stirred at room temperature for 5 min, and then nickel nitrate solution was added with continuous stirring. The excess water in the resulted precursor solutions was removed from each sample by heating the samples to 383 K with occasional stirring. The dried samples were then calcined in air at 773 K for 5 h and, finally, reduced in a flow of pure H₂ (1000 mL·g⁻¹·min⁻¹) at 923 K for 2.5 h (for Ni₂P, 823 K). The samples were cooled to room temperature in flowing H₂. Before being exposed to air, they were passivated under a flow of 1.0 vol % O₂/Ar for 24 h. Details of the characterization can be found in note 10.

Figure 1 shows the XRD patterns of nominal compositions MoP, Ni_{0.4}Mo_{1.6}P_{1.6}, Ni_{0.66}Mo_{1.34}P_{1.34}, NiMoP, Ni_{1.34}Mo_{0.66}P, Ni_{1.6}Mo_{0.4}P, and Ni₂P. The XRD results of MoP, Ni₂P, and NiMoP agree well with the reference

* To whom correspondence should be addressed.

[†] Oxford University.

[‡] University of St. Andrews.

[§] Fudan University.

^{||} E-mail: Malcolm.Green@chemistry.oxford.ac.uk.

(1) Topsoe, H.; Clausen, B. S. *Catal. Rev.-Sci. Eng.* **1984**, *26*, 395.
Oyama, S. T. *The Chemistry of Transition Metal Carbides and Nitrides*; Oyama, S. T., Ed.; Blackie Academic & Professional: Scotland, 1996.
(2) Djega-Mariadassou, G.; Boudart, M.; Bugli, G.; Sayag, C. *Catal. Lett.* **1995**, *31*, 411. Park, K. Y.; Seo, W. K.; Lee, J. S. *Catal. Lett.* **1991**, *11*, 349.

(3) York, A. P. E.; Claridge, J. B.; Brungs, A. J.; Tsang, S. C.; Green, M. L. H. *Chem. Commun.* **1997**, 39. Claridge, J. B.; York, A. P. E.; Brungs, A. J.; Marquez-Alvarez, C.; Sloan, J.; Tsang, S. C.; Green, M. L. H. *J. Catal.* **1998**, *180*, 85.

(4) Li, W.; Bhandappani, B. B.; Oyama, S. T. *Chem. Lett.* **1998**, 207.
(5) Oyama, S. T.; Clark, P.; Teixeira da Silva, V. L. S.; Lede, E. J.; Requero, F. G. *J. Phys. Chem. B* **2001**, *105*, 4961. Clark, P.; Li, W.; Oyama, S. T. *J. Catal.* **2001**, *200*, 140. Clark, P.; Wang, X.; Oyama, S. T. *J. Catal.* **2002**, *207*, 256.

(6) (a) Stinner, C.; Prins, R.; Weber, Th. *J. Catal.* **2000**, *191*, 438.
(b) Stinner, C.; Tang, Z.; Houas, M.; Weber, Th.; Prins, R. *J. Catal.* **2002**, *208*, 456.

(7) Phillips, D. C.; Sawhill, S. J.; Self, R.; Bussell, M. E. *J. Catal.* **2002**, *207*, 266.

(8) Stinner, C.; Prins, R.; Weber, Th. *J. Catal.* **2001**, *202*, 187.

(9) Stanislaus, A.; Cooper, B. H. *Catal. Rev.-Sci. Eng.* **1994**, *36*, 75.

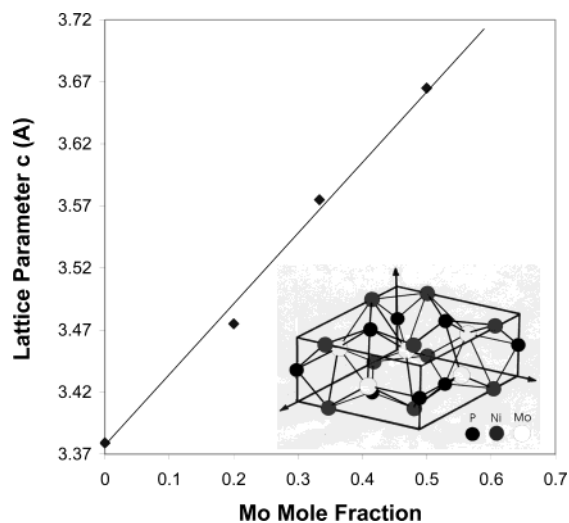


Figure 2. A linear relationship of the lattice parameter c of $\text{Ni}_{(2-x)}\text{Mo}_x\text{P}$ ($x = 0-1$) solid as a function of molybdenum mole fractions, which is measured from XRD patterns (square data points), is observed. Inset is the structural model of NiMoP (Fe_2P type).

patterns¹¹ and the recent report by Weber and co-workers.⁸ The XRD pattern of MoP shows peaks at 28.0, 32.2, 43.2, 57.3, 64.9, and 67.4°. The addition of nickel decreases the intensities of peaks ascribed to MoP and leads to the appearance of new X-ray diffraction peaks at 30.1, 39.4, 40.5, 44.5, 47.3, 54.0, and 66.3° (Figure 1b). Certainly a phase separation happened here. These peaks can be attributed to a mixture of Ni_2P and NiMoP . With an increase of the Ni content (Figure 1c), the MoP diffraction peaks were again weakened, while those of NiMoP and Ni_2P become more intense. Further increase

in the nickel content results in the formation of a pure NiMoP phase, at $\text{Ni}/\text{Mo} = 1$ (Figure 1d). NiMoP has an Fe_2P -type hexagonal structure (see inset of Figure 2 of NiMoP structure) with a space group of $P6_2m$ (189) and unit cell parameters $a = 5.861 \text{ Å}$ and $c = 3.704 \text{ Å}$.¹¹ Accordingly, the peaks at 30.1, 39.3, 43.3, 47.3, 49.5, 54.1, and 66.3° correspond to the (110), (111), (201), (210), (002), (300), and (310) planes, respectively.

When the ratio of Ni/Mo is greater than 1, the XRD patterns of the samples are very similar and some peaks are shifted to higher angles while others are unchanged (Figure 1e,f). We noticed that all the shifted peaks have Miller indexes with $l \neq 0$ and all the unchanged peaks have $l = 0$. This indicates that the lattice parameter c decreases with the increase of Ni until the composition approaches Ni_2P , which has also an Fe_2P -type structure with $a = 5.859 \text{ Å}$ and $c = 3.382 \text{ Å}$.¹¹ This is strong evidence for the presence of solid solutions in this range. For all the samples investigated ($\text{Ni}_{(2-x)}\text{Mo}_x\text{P}$ ($x = 0-1$)), the lattice parameters a and b measured from XRD patterns remain almost constant (from 5.86 to 5.866 Å). However, as shown in Figure 2, the lattice parameter c exhibits a nearly linear relationship with the Mo compositions. A gradual increase in the lattice parameter c is observed as the Mo composition increases. This trend is consistent with Vegard's law, indicating that Ni is likely to be homogeneously substituted. Furthermore, all the peaks become sharper with the increase of the Ni/Mo ratio, indicating that the crystallite size of the sample becomes larger with the addition of nickel.

The presence of solid solutions in $\text{Ni}_{(2-x)}\text{Mo}_x\text{P}$ was confirmed by EDX and HRTEM investigations. In the EDX studies, Ni $K\alpha$, Mo $L\alpha$, and P $K\alpha$ peaks were used in the calculation of the compositions. It was found that

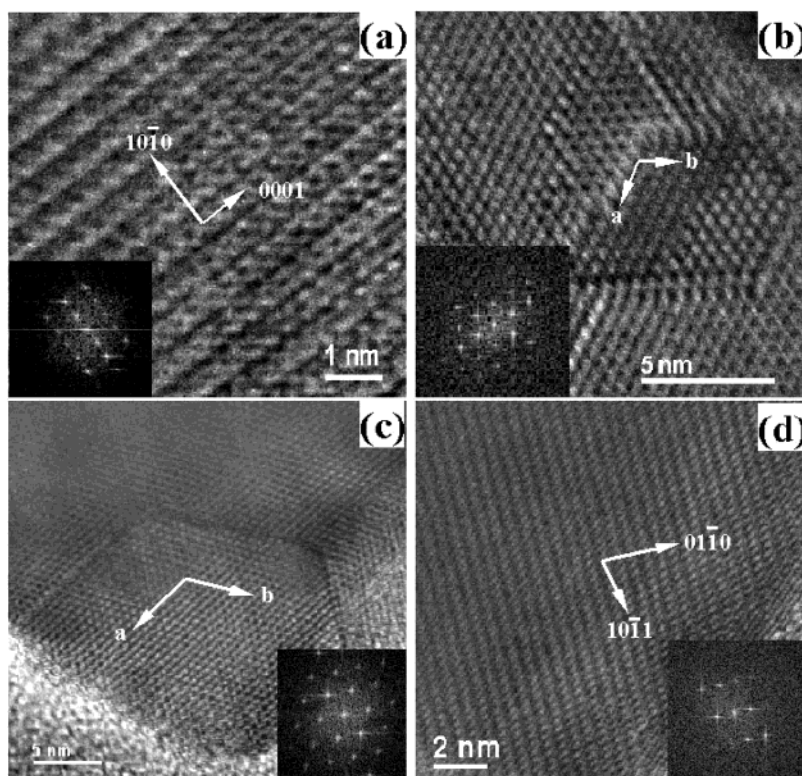


Figure 3. HRTEM images and corresponding Fourier transform diffraction patterns from the solid solutions: (a) NiMoP viewed down the $[0110]$ zone axis, (b) $\text{Ni}_{1.34}\text{Mo}_{0.66}\text{P}$ on the $[0001]$ projection, (c) $\text{Ni}_{1.6}\text{Mo}_{0.4}\text{P}$ on the $[0001]$ projection, and (d) Ni_2P along the $[1011]$ direction.

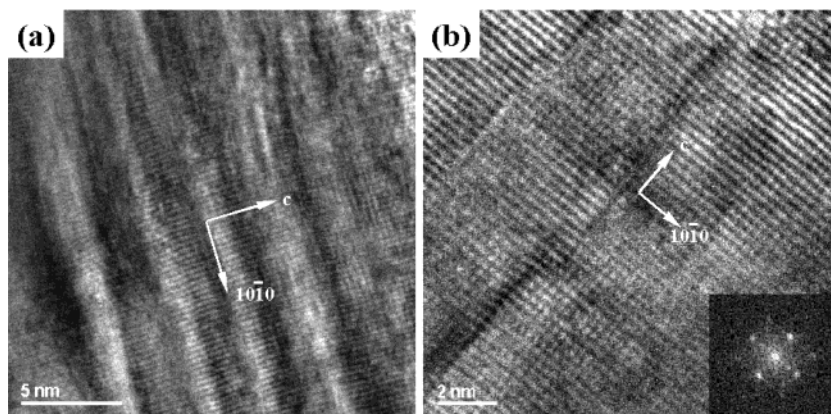


Figure 4. HRTEM images along the $[11\bar{2}0]$ zone axis of MoP, showing (a) irregular superlattices along the c axis and (b) antiphase grain boundaries.

the ratios of Ni:P and Mo:P at all the points of each sample were almost constant for each sample and varied accordingly with their nominal compositions. The EDX results of the specimens, collected from about 10 individual particles for each specimen, were calibrated to be $\text{Ni}_{2.01} \pm 0.18\text{P}_{0.99}$ for the sample with a nominal composition of Ni_2P , $\text{Ni}_{1.59} \pm 0.16\text{Mo}_{0.47} \pm 0.06\text{P}_{0.96}$ for $\text{Ni}_{1.6}\text{Mo}_{0.4}\text{P}$, $\text{Ni}_{1.37} \pm 0.08\text{Mo}_{0.62} \pm 0.05\text{P}_{1.02}$ for $\text{Ni}_{1.34}\text{Mo}_{0.66}\text{P}$, and $\text{Ni}_{1.00} \pm 0.06\text{Mo}_{0.95} \pm 0.03\text{P}_{1.05}$ for NiMoP . The ratio of Ni:Mo can be changed continuously indeed in the compositional range of $\text{Ni}_{(2-x)}\text{Mo}_x\text{P}$ with $x = 0-1$. Figure S1 shows EDX spectra of specimens of $\text{Ni}_{1.34}\text{Mo}_{0.66}\text{P}$ and $\text{Ni}_{1.6}\text{Mo}_{0.4}\text{P}$ (see Supporting Information).

HRTEM data further support the conclusion of solid solutions in the compositional range of $\text{Ni}_{(2-x)}\text{Mo}_x\text{P}$ ($x = 0-1$). Figure 3 shows typical images from four compositions of such solid solutions prepared in the present work. HRTEM images from both end members of solid solutions, Ni_2P and NiMoP , show an Fe_2P structure with unit cell parameters similar to those in the literature data.¹¹ A similar phenomenon was also observed from HRTEM images of the other two compositions, $\text{Ni}_{1.34}\text{Mo}_{0.66}\text{P}$ and $\text{Ni}_{1.6}\text{Mo}_{0.4}\text{P}$, with the c axes being between those of the end members. No superstructures were observed from all the images viewed

down various zone axes, indicating that Ni and Mo atoms are randomly distributed over the metal sites of the Fe_2P structure. Only when viewed down the $[0001]$ zone axis were some domain structures observed (Figure 3b,c). The formation of the domains is based on a layer shifting along the **a** and **b** directions. Since there are some (100) and (010) atomic planes containing only cations and some containing only anions, a small variation of the composition can be expected.

Figure 4 shows two typical images from MoP when viewed down the $[11\bar{2}0]$ zone axis of the hexagonal unit cell with $a = 3.231 \text{ \AA}$ and $c = 3.207 \text{ \AA}$. Irregular superlattices along the c axis were commonly seen in the sample (Figure 4a). The EDX examination indicated that the sample was homogeneous with an average composition of $\text{Mo}_{1.07} \pm 0.08\text{P}_{0.93}$ from 12 particles. Figure 4b shows antiphase grain boundaries. In the structure of MoP, both Mo and P are 6-coordinated and can change the sites to form antiphase domains. This type of defect will not change the composition.

In conclusion, solid solution materials with the formula $\text{Ni}_{(2-x)}\text{Mo}_x\text{P}$ ($x = 0-1$) have been prepared and shown to belong to Fe_2P type. Under such a general formula, the cation ratio of Ni/Mo can be freely changed, thus enabling us to modify the anticipated catalytic properties.

Acknowledgment. D. Ma thanks the Royal Society for a postdoctoral fellowship and K. Perkin for reading through the manuscript.

Supporting Information Available: EDX spectra of specimens of $\text{Ni}_{1.34}\text{Mo}_{0.66}\text{P}$ and $\text{Ni}_{1.6}\text{Mo}_{0.4}\text{P}$. This material is available free of charge via the Internet at <http://pubs.acs.org>.

CM035233E

(10) XRD of the samples were scanned on a Philips PW1710 diffractometer with Cu K α radiation. A high-resolution transmission electron microscopic (HRTEM) investigation was performed on a JEOL JEM-2011 electron microscope. Energy-dispersive X-ray microanalysis (EDX) was carried out using an Oxford ISIS system attached to the same microscope. Specimen for the HRTEM and EDX studies was prepared by dispersing the powder in acetone with an ultrasonic treatment for about 1 min. One drop of suspension was then deposited on a copper grid with a holey carbon film. The specimen grid was allowed to dry in air before being transferred into the specimen chamber of the microscope.

(11) PDF 24-771 (MoP); PDF 74-1385 (Ni_2P); PDF 31-0873 (NiMoP).